Developmental Cell, Vol. 2, 411–423, April, 2002, Copyright ©2002 by Cell Press

GPI-Anchored Proteins Are Delivered to Recycling Endosomes via a Distinct cdc42-Regulated, Clathrin-Independent Pinocytic Pathway

Shefali Sabharanjak,[1,4] Pranav Sharma,[1,4] Robert G. Parton,[2] and Satyajit Mayor[1,3]
[1] National Centre for Biological Sciences
UAS-GKVK Campus
Bellary Road
Bangalore, 560 065
India
[2] Institute for Molecular Bioscience
Centre for Microscopy and Microanalysis and
School of Biomedical Sciences
University of Queensland
Queensland, 4072
Australia

Summary

Endocytosis of cell-surface proteins via specific pathways is critical for their function. We show that multiple glycosylphosphatidylinositol-anchored proteins (GPI-APs) are endocytosed to the recycling endosomal compartment but not to the Golgi via a nonclathrin, noncaveolae mediated pathway. GPI anchoring is a positive signal for internalization into rab5-independent tubular-vesicular endosomes also responsible for a major fraction of fluid-phase uptake; molecules merely lacking cytoplasmic extensions are not included. Unlike the internalization of detergent-resistant membrane (DRM)-associated interleukin 2 receptor, endocytosis of DRM-associated GPI-APs is unaffected by inhibition of RhoA or dynamin 2 activity. Inhibition of Rho family GTPase cdc42, but not Rac1, reduces fluid-phase uptake and redistributes GPI-APs to the clathrin-mediated pathway. These results describe a distinct constitutive pinocytic pathway, specifically regulated by cdc42.

Introduction

The GPI moiety is the sole membrane anchor for a large and heterogeneous group of cell-surface proteins with diverse functions, including enzymes, immune antigens, parasite antigens, and receptors (Ferguson, 1999). The presence of the GPI anchor and endocytosis of the GPI-anchored proteins (GPI-AP) appears necessary for the function or pathology of many of these proteins. Internalization into acidic compartments is necessary for folate uptake via the folate receptor (FR-GPI) (Kamen et al., 1991) and for the cellular prion protein (PrP^{c}) to get converted into infectious scrapie (PrP^{sc}) particles (Borchelt et al., 1992). Replacement of the GPI anchor with transmembrane protein sequences containing clathrin pit-localization motifs results in reduced folate uptake (Ritter et al., 1995) and scrapie conversion (Kaneko et al., 1997; Taraboulos et al., 1995). Furthermore, GPI-APs are often receptors for numerous viruses and bacterial toxins (Bergelson et al., 1994; Chan et al., 2001; Diep et al., 1998; Ricci et al., 2000). Therefore, understanding endocytic pathways and mechanisms of GPI-AP internalization is critical.

There is no general consensus regarding the internalization process or endocytic pathway of GPI-APs, although a number have been studied in different cell types (reviewed in Chatterjee and Mayor, 2001). GPI-APs have been postulated to participate in an endocytic process involving caveolae, termed potocytosis (Anderson et al., 1992). However, several studies have shown that GPI-APs are not concentrated in caveolae or clathrin-coated pits; they are localized to caveolae *only* after crosslinking induced by multivalent antibodies (Fujimoto, 1996; Mayor and Maxfield, 1995; Mayor et al., 1994; Parton et al., 1994). Internalization of some GPI-APs was shown to be pharmacologically or kinetically different from that of transmembrane proteins (reviewed in Chatterjee and Mayor, 2001). In some studies, GPI-APs entered morphologically different compartments, compared to transmembrane counterparts internalized via clathrin pits. In several studies, multivalent ligands were used to study the route of internalization of the GPI-AP. In studies where monovalent ligands were used to trace their endocytic pathway, multiple GPI-APs have been detected in the same endocytic compartments as internalized markers of the fluid-phase (Chatterjee et al., 2001; Mayor et al., 1998; Rijnboutt et al., 1996) and in the recycling endosomal compartment (RE) (Chatterjee et al., 2001; Mayor et al., 1998). In contrast, Nichols et al. (2001) suggest that multiple GFP-tagged GPI-APs (GPI-GFPs) are endocytosed directly to the Golgi.

Given their uniform, diffuse distribution at the cell surface (Mayor and Maxfield, 1995; Mayor et al., 1994; Parton et al., 1994), GPI-APs may be internalized by any of the multiple routes of endocytosis available (Lamaze and Schmid, 1995; Mukherjee et al., 1997). GPI-APs are likely to be internalized via dynamin (dyn) and clathrin-independent means since inhibitors of dyn and clathrin do not inhibit uptake of toxins internalized via GPI-anchored toxin receptors (Ricci et al., 2000; Skretting et al., 1999). Nichols et al. (2001) used alterations in the kinetics and extent of Golgi delivery of GPI-GFPs to argue that GPI-APs in Cos-7 cells are internalized via a clathrin-independent mechanism bypassing the conventional rab5-regulated endocytic pathway. Since GPI-APs are known to be associated with detergent-resistant membranes (DRMs), another likely route is the clathrin-independent RhoA-regulated pathway followed by DRM-associated interleukin receptors, IL2-R (Lamaze et al., 2001).

To directly address the endocytic pathway taken by GPI-APs, we have examined early steps in the internalization of the folate receptor (FR-GPI), decay-accelerating factor (DAF), and GPI-GFP (Nichols et al., 2001) in CHO and Cos-7 cells. In addition, we have studied cell types that endogenously express FR-GPI. Using quantitative fluorescence microscopy and electron microscopy (EM), we provide evidence that GPI-APs tagged with monovalent ligands are selectively endocytosed via

[3] Correspondence: mayor@ncbs.res.in
[4] These authors contributed equally to this work.

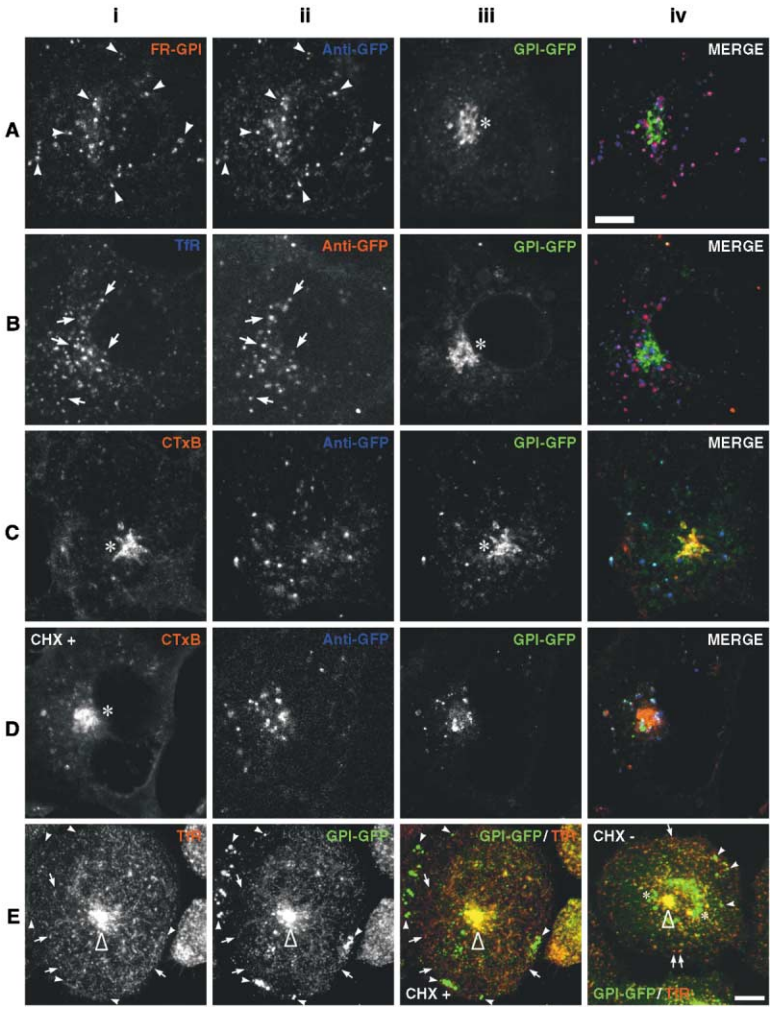

Figure 1. Multiple GPI-APs Are Delivered to the RE in COS and CHO Cells

(A–D) Cos-7 cells were incubated for 1 hr at 37°C in the absence (A–C) or presence of pretreatment with cycloheximide (D) for 5 hr at 37°C. In (A) cells were incubated with Alexa568-FabMOv19 (i; red in iv) and Cy5-anti-GFP mAb (ii, blue in iv). In (B) cells were incubated with Cy5-Tf (i; blue in iv) and Alexa568-anti-GFP (ii; red in iv). In (C) and (D) cells were incubated with Cy3-CTxB (i, red in iv) and Cy5-anti-GFP (ii, blue in iv). Cells were imaged for appropriate fluorophores using a confocal microscope. Single confocal planes are shown as grayscale images (i–iii) and their triple color merges (iv) to indicate the extent of colocalization of the endocytosed probes with endogenous GPI-GFP fluorescence (iii; green in iv). Arrowheads (A) indicate FR-GPI-containing structures; internalized Tf is marked by arrows (B).

(E) CHO cells expressing GPI-GFP (GG8Tb-1 cells) were treated (3 hr at 37°C) with (i–iii) or without (iv) CHX, labeled with A568-Tf for 20 min at 37°C, and imaged on a confocal microscope. GPI-GFP (ii; green in iii and iv) is present in peripheral compartments (arrowheads) devoid of Tf (i; red in iii and iv) but is colocalized with Tf in the perinuclear RE (open triangle). Tf-containing peripheral endosomes are indicated by arrows. Golgi is indicated by asterisks in all panels.

Bar in (A) (for [A–D]) and (E), 10 μm.

a nonclathrin, noncaveolar, and dynamin-independent pinocytic pathway to the RE and are not delivered to the Golgi. This pathway is selective for GPI-APs; molecules merely lacking clathrin localization motifs are not included. Unlike the IL2-R pathway, GPI-AP internalization is regulated by the small GTPase cdc42, but not by RhoA.

Results

Multiple GPI-APs Including GPI-GFP Are Delivered to the RE but Not to the Golgi in Different Cell Types

Recent studies have suggested that GFP-tagged GPI-APs, GFP attached to the GPI-anchoring signal of FR and GFP-tagged CD59 are delivered to the Golgi in Cos-7 cells, whereas FR-GPI is internalized into transferrin (Tf)-containing endosomes (Nichols et al., 2001). These results are contrary to previous observations in CHO cells which state that two different GPI-APs, FR-GPI and DAF, are delivered to the RE (Chatterjee et al., 2001; Mayor et al., 1998). To address the reason for this discrepancy, the endocytic destinations of GPI-GFP in Cos-7 cells were examined by using fluorescently conjugated monoclonal antibodies (1B3A8) directed against the GFP moiety (Fl-anti-GFP). We find that Fl-anti-GFP is delivered to endocytic compartments accessible to cointernalized antibodies against coexpressed FR-GPI (Figure 1A). A majority of these compartments in the perinuclear region are also accessed by endocytosed Tf, a marker of the RE (Figure 1B) that is not delivered to the Golgi (see Supplemental Data, Figure S1 [http://www.developmentalcell.com/cgi/content/full/2/4/411/DC1]). Although endocytosed Fl-anti-GFP is detected in the RE, it is not delivered to the Golgi as identified by cointernalized cholera toxin B subunit (CTxB; Figure 1C). If GPI-APs are delivered to the Golgi via the endocytic pathway (Nichols et al., 2001), inhibition of protein synthesis by cycloheximide (CHX) should not completely clear the Golgi pool of GPI-GFP in Cos-7 cells. Contrary to Nichols et al. (2001), we find that that CHX treatment for 4–5 hr completely removes Golgi-localized GPI-GFP fluorescence in a large fraction (~60%) of cells (Figure 1D). At the same time, CTxB continues to be delivered to the Golgi (Figure 1D). Golgi localization of CTxB was confirmed by colocalization with a bona fide Golgi marker, C_6-NBD-Ceramide (see Supplemental Data, Figure S1). In untreated cells, a major fraction of endogenous GPI-GFP fluorescence in the perinuclear region (Figures 1A–1C) is colocalized with endocytosed CTxB in the Golgi (Figure 1C; Nichols et al., 2001). However, this pool remains inaccessible to endocytosed Fl-anti-GFP (Figures 1A–1C). In CHX-treated cells, the lack

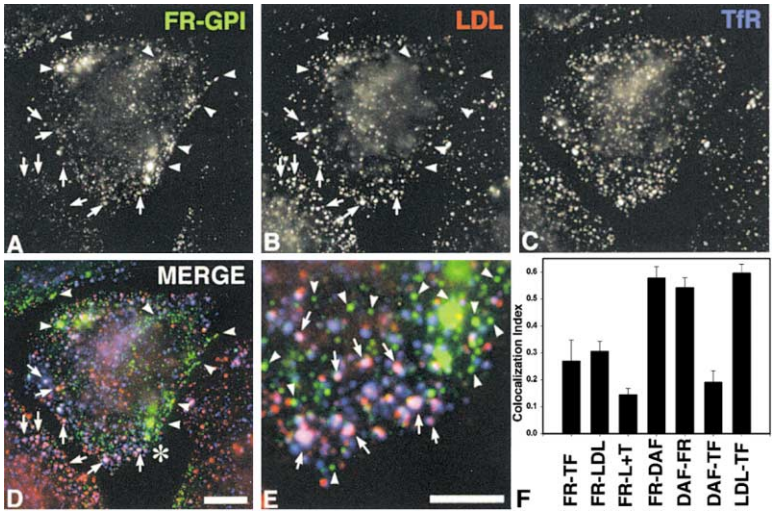

Figure 2. GPI-APs Are Internalized into Endosomes Devoid of Tf and LDL

(A–E) FRαTb-1 cells were labeled with Alexa488-Fab-MOv18 (A), DiI-LDL (B), and Cy5-Tf (C) for 2 min at 37°C and imaged on a high-resolution wide-field microscope. Images of FR-GPI (green), Tf (blue), and LDL (red) were pseudocolored and color merged (D and E). GPI-AP-enriched endosomes (GEECs; [A–E], arrowheads) are quite distinct from sorting endosomes containing internalized LDL and Tf ([A–E], arrows). (E) shows a magnified view of the region corresponding to the asterisk in (D).

(F) Histogram showing the fraction of colocalized intensity of GPI-APs cointernalized with endocytic tracers, Tf and LDL. The image used as the reference image is indicated after the hyphen. FR-L + T indicates colocalization of FR-GPI in endosomes containing both TfR and LDL.

Bars, 10 μm (D), and 5 μm (E).

of Golgi localization of GPI-GFP is observed in a similar fraction of cells (~60% ± 10%), irrespective of the presence (Figure 1D) or absence (data not shown) of endocytosed antibody, confirming that incubation with Fl-anti-GFP does not affect GPI-GFP distribution and trafficking. In this fraction of CHX-treated Cos-7 cells, all the endogenous GPI-GFP becomes accessible to endocytosed Fl-anti-GFP (compare Figures 1Dii and 1Diii). The non-Golgi-localized GPI-GFP pool is unaffected by CHX treatment (compare Figures 1C and 1D), incubation with antibodies (data not shown), or treatment with brefeldin A (data not shown).

In CHO cells, CHX treatment results in a loss of Golgi-localized GPI-GFP fluorescence in almost all cells (>90%); the remnant perinuclear GFP fluorescence is completely colocalized with cointernalized Tf in the RE (Figure 1E, i–iii, open triangle). In the absence of CHX treatment, endocytosed anti-GFP and FR-GPI antibodies also remain completely colocalized (see Supplemental Data, Figure S2 [http://www.developmentalcell.com/cgi/content/full/2/4/411/DC1]). Furthermore, similar to previous studies with FR-GPI and DAF (Mayor et al., 1998), the fluorescence of perinuclear GPI-GFP in CHX-treated CHO cells is completely quenched by cointernalized HRP-Tf (see Supplemental Data, Figure S2), confirming that GPI-GFP is present in the RE. In untreated cells in addition to the RE, GPI-GFP is observed in a perinuclear Golgi compartment (Figure 1E, iv), which is redistributed by treatment with brefeldin A (see Supplemental Data, Figure S3).

The persistence of Golgi-associated GPI-GFP fluorescence in a fraction of CHX-treated Cos-7 cells is likely to be due to the incomplete emptying of a large pool of GFP moieties visualized in the endoplasmic reticulum in Cos-7 cells. These results provide an explanation for the data obtained by Nichols et al. (2001) (discussed in detail in Supplemental Data [http://www.developmentalcell.com/cgi/content/full/2/4/411/DC1]). These results, along with electron microscopy (EM) data depicting the lack of Golgi delivery of endocytosed anti-GFP gold antibodies (Figure 3M), confirm that multiple GPI-APs in different cell types are delivered to the RE but not to the Golgi.

GPI-APs Are Internalized into Endosomes Devoid of Markers of the Clathrin-Dependent Pathway

Although multiple GPI-APs are extensively colocalized with endocytosed Tf in the RE (Figure 1; Mayor et al., 1998), a substantial fraction (30% of FR-GPI in CHO cells) of the internalized GPI-AP pool remains consistently segregated from Tf (Mayor et al., 1998) and the Golgi (see Supplemental Data, Figure S3 [http://www.developmentalcell.com/cgi/content/full/2/4/411/DC1]). This was determined by quantitative (Mayor et al., 1998) and qualitative (see Supplemental Data, Figure S2) analyses of (HRP-mediated) quenching of fluorescently labeled reagents for GPI-APs by coendocytosed HRP-Tf. To determine whether this segregation is due to internalization of GPI-APs via a distinct endocytic pathway, we have directly examined early steps in the endocytosis of GPI-APs in comparison with markers of the clathrin-mediated pathway, Tf and LDL, internalized via their respective receptors. Immediately after internalization (2 min), a majority of endocytosed FR-GPI is present in mainly small and some large-sized endosomes (Figures 2A–2E, arrowheads; see also magnified region in Figure 2E), clearly separate from those containing internalized Tf and LDL (Figures 2A–2E, arrows). Lysosomally destined LDL is extensively colocalized with Tf in sorting endosomes at this time (Figures 2A–2E, arrows; Dunn et al., 1989; Mayor et al., 1993). FR-GPI-containing endosomes are often found in distinct regions of the cell (Figures 2A–2E, arrowheads; see also Figure 4). Quantitative analysis (Figure 2F) of the extent of colocalization shows that a majority of FR-GPI fluorescence at these times (~70%) does not overlap with Tf- or LDL-labeled endosomes; only 13% of FR-GPI is colocalized with sorting endosomes defined by the combined presence of Tf and LDL. At this time, ~60% of LDL is colocalized with coendocytosed Tf. Qualitatively similar separation of endocytosed FR-GPI and clathrin-dependent markers are seen at times as short as 1 min after internalization (data not shown). Identical segregation of FR-GPIs and TfR is also observed when monovalent fluorescent folate analogs, N^{α}-pteroyl-N^{ϵ}-(4′-fluorescein-thiocarbamoyl)-L-lysine or N^{α}-pteroyl-N^{ϵ}-(4′-lissamine rhodamine-thiocarbamoyl)-L-lysine (PLF or PLR; data not

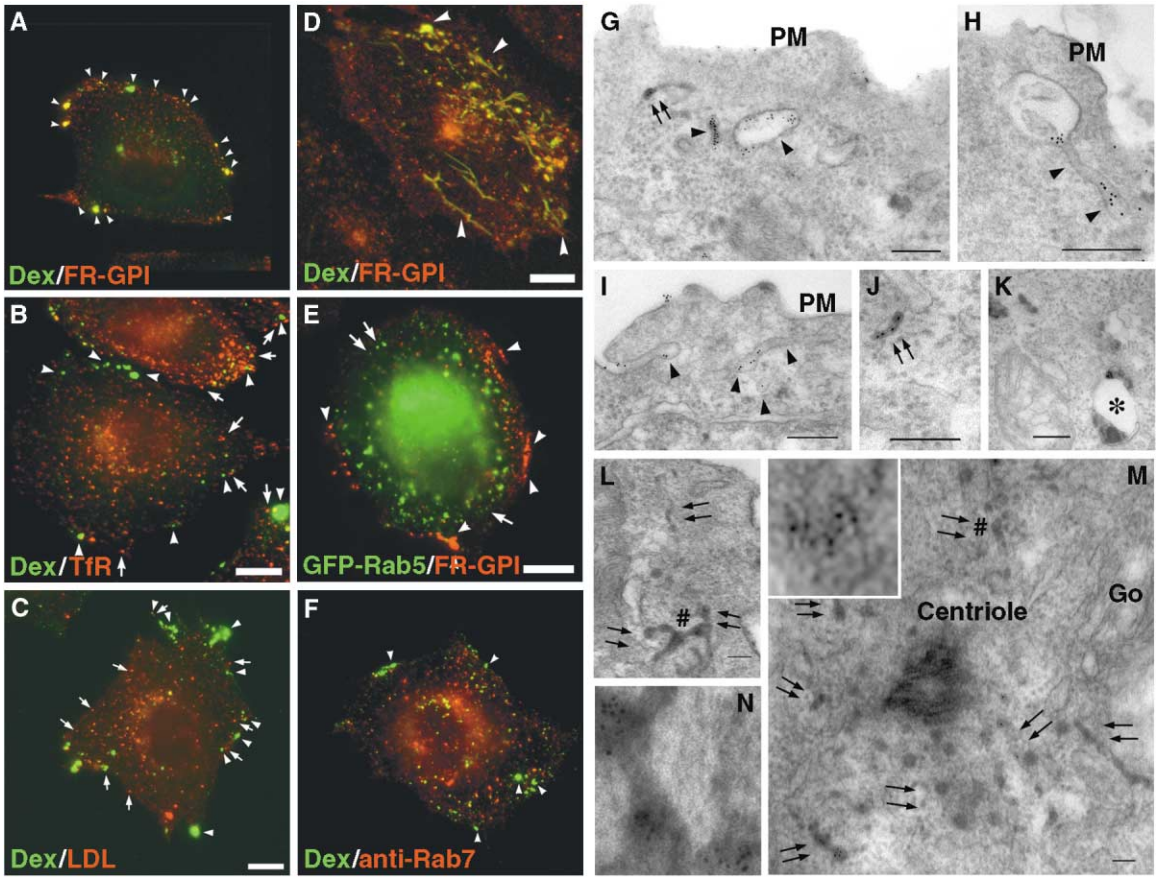

Figure 3. GPI-APs Are Internalized into Distinct Early Endosomes along with a Major Fraction of the Fluid-Phases

(A–D) FRαTb-1 cells were incubated for 2 min (A and B), 5 min (C), or 20 min (D) with F-Dex (1 mg/ml, [A–D]), Cy5-FabMOv19 (A), Alexa568-Tf (B), DiI-LDL (C), and PLR (D) at 37°C, and fixed cells (A–C) were imaged on a wide-field microscope or live (D) on a confocal microscope.
(E) FRαTb-1 cells expressing GFP-rab5 (green) were labeled with Cy5-FabMOv19 (red) for 2 min at 37°C and imaged as in (A).
(F) FRαTb-1 cells were incubated with F-Dex (green) for 5 min at 37°C and immunostained for rab7 (red). Arrowheads denote F-Dex and FR-GPI-labeled compartments; arrows denote Tf-, LDL-containing or rab7-marked endosomes. Bars, 10 μm.
(G–N) Electron microscopic examination of GPI-GFP internalization. GPI-GFP-expressing cells were incubated with 5 nm anti-GFP gold together with HRP (10 mg/ml). After various times at 37°C (20 min, [G], [L], and [M]; 5 min, [H–K]), the cells were washed to remove surface HRP and processed for EM. Fifty (G–K) or 200 nm (L–N) sections were viewed unstained to facilitate visualization of HRP and gold particles. Gold particles are observed within HRP-containing tubular structures close to the plasma membrane (PM; [G], [J], and [L], small double arrow) and the centriole (M). (N) and inset in (M) show a magnification (4× and 90° clockwise rotation in [N]; 10× in [M]) of the region marked by a pound sign (#) in (L) and (M), respectively, to visualize the 5 nm anti-GFP gold particles in DAB-stained structures observed in thick section. Some HRP-negative structures are surface connected (large arrowheads) and show concentration of the probe as compared to the plasma membrane proper (PM) in the same cell (G–I). Gold particles and HRP also colocalize in characteristic sorting endosomes (asterisk). Gold particles are not detected in putative Golgi elements ("Go" in [M]).
Bars, 200 nm.

shown) or monovalent Fab fragments were used to visualize the endocytic pathway of FR-GPI. In subsequent experiments, we have used the more intensely fluorescent Fab fragments as monovalent ligands to study the trafficking of different GPI-APs. The segregation of GPI-APs from TfR is not specific to FR-GPI; a majority of another cointernalized GPI-anchored protein, DAF, is also extensively colocalized with FR-GPI but not with TfR at 2 min in the same cells (Figure 2F). Together, these data show that immediately after internalization (<2 min), a major fraction of GPI-APs is present in compartments distinct from TfR-containing endosomes. These compartments have been termed GEECs (GPI-AP enriched early endosomal compartments).

Endocytosed GPI-APs Colocalize with Fluid-Phase Markers in rab5-Independent Acidic Pinosomes

To determine whether other endocytic probes may be internalized into GEECs, we examined the distribution of internalized FITC-conjugated Dextran (F-Dex) and Lucifer yellow (LY). At a low concentration (1 mg/ml), the majority of F-Dex (Figure 3A) and LY (data not shown), immediately after internalization are colocalized with FR-GPI (Figure 3A, arrowheads) but not with endosomes marked by cointernalized Tf (Figure 3B, arrows), or DiI-LDL (Figure 3C, arrows). At later times (20 min) in living cells these F-Dex-filled endosomes often have an extensive tubular vesicular morphology, colocalizing with endocytosed FR-GPI (Figure 3D), GPI-GFP (Supplemental

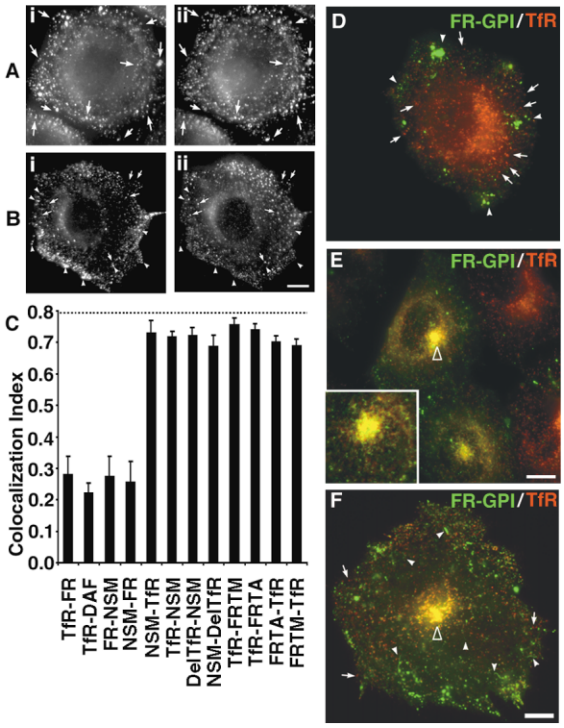

Figure 4. GPI-APs Are Specifically Delivered to GEECs Prior to Their Delivery to the RE

(A–C) Cells expressing FR isoforms, transmembrane FR-TA (A), or FR-GPI (B) were incubated for 2 min at 37°C with PLR (A, i) and Oregon green-Tf (A, ii), or Alexa568-FabMOv18 (B, i), C_6-NBD-SM (B, ii) to visualize the extent of colocalization between the endocytosed probes as described in Figure 2. Histogram (C) shows the quantitative extent of reciprocal colocalization between TfR, FR-GPI (FR), DAF, FR-TM (FRTM), FR-TA (FRTA), C_6-NBD-SM (NSM), and δ3-59TfR (DelTfR). The image used as the reference image is indicated after the hyphen as described in Figure 1F. Maximum colocalization observed between cointernalized Alexa568- and Cy5-labeled Tf is indicated by the dotted line in (C).

(D–F) FRαTb-1 cells were labeled with Alexa488-FabMOv18 (green) and Alexa568-Tf (red) for 2 min (D and E) or 20 min (F), and imaged on a wide-field microscope immediately (D) or after a 10 min chase at 37°C (E) after fixation, or live on a confocal microscope (F). FR-GPI (arrowheads in [D] and [F]) and TfR (arrows in [D] and [F]) are included in distinct sets of endosomes at early times (D) and then delivered to the RE (open triangle in [E] and [F]). Inset shows colocalization between the two receptors in the RE as observed in a confocal microscope. FR-GPI enriched endosomes (F) show a tubular vesicular morphology in living cells (arrowheads) distinct from the Tf-containing endosomes (arrows).

Bars, 10 μm.

Data [http://www.developmentalcell.com/cgi/content/full/2/4/411/DC1]), and DAF (Mayor et al., 1998); a small fraction of F-Dex also reaches the pericentriolar RE (Figure 3D). The morphology of GEECs is extremely sensitive to cold treatment and fixation with paraformaldehyde, resulting in a globular structure (compare Figures 3A–3C with 3D). Using 10-fold higher concentrations of the fluid-phase probe, in addition to the GEECs, F-Dex is also detected in compartments containing Tf at early times (data not shown).

Consistent with the lack of colocalization with endocytosed Tf and LDL, GEECs (containing FR-GPI or F-Dex) do not colocalize with compartments marked by GFP-rab5 (Figure 3E), GFP-rab4 (data not shown), or antibodies to rab7 (Figure 3F). GFP-rab4 and rab5 colocalize with Tf in sorting endosomes at these times (data not shown; Sonnichsen et al., 2000). GEECs were persistent in CHO cells overexpressing wild-type GFP-rab5, dominant-negative GFP-rab5S34N or active GFP-rab5Q79L, although GFP-rab5Q79L perturbed the morphology of TfR-containing sorting endosomes as expected (data not shown). These experiments rule out a role for rab5 in the formation of GEECs, indicating that these endosomes are distinct from the classical clathrin pit-derived sorting endosomes.

The GEECs are acidic compartments because fluorescence of the pH-sensitive F-Dex (Ohkuma and Poole, 1978), pulsed into cells for 2, 5, or 20 min, is significantly enhanced upon neutralizing endosomal pH with the K^+ ionophore, nigericin, in living cells (data not shown). To ascertain whether GEECs are induced by ectopic expression of GPI-APs in CHO cell lines, we examined the distribution of internalized F-Dex and Tf in the parent CHO line, TRVb-1. In these cells, F-Dex is also included in tubular-vesicular endosomes not colocalized with TfR (data not shown). In cells (KB cells) that endogenously express GPI-APs, FR-GPI is also internalized into TfR-independent compartments (data not shown). These data confirm that GEECs are neither induced nor aberrant endocytic compartments.

We next examined by EM the earliest steps in GPI-GFP internalization in experiments wherein anti-GFP-gold was added together with HRP (10 mg/ml) as a fluid-phase marker for various times at 37°C; alternatively, Tf-HRP was added as a specific marker of the clathrin-coated pit pathway. Anti-GFP-gold colocalized with HRP-labeled structures at 5 min (Figures 3I–3K) and 20 min (Figures 3G, 3H, and 3L–3N) in tubular elements of ~28–40 nm in diameter (double small arrows), as well as in readily identifiable, ring-shaped cisternal putative early sorting endosomes (Figure 3K, asterisk), which are also labeled by Tf-HRP (data not shown). The extensive tubular morphologies are better visualized in 200 nm thick section EM (Figure 3L–3N). There was also a striking labeling of anti-GFP-gold within HRP-negative tubular elements, which were clearly surface connected (Figure 3I). The gold density appeared higher in these elements than on the bulk plasma membrane, consistent with specific sorting of GPI-APs in these structures (Figures 3G–3I, large arrowheads). These structures are the likely precursors of the GEECs observed by light microscopy. Consistent with this, Tf-HRP predominantly labeled early sorting endosomes with little overlap with anti-GFP-gold in the characteristic tubular elements (data not shown). Gold particles are not detected in putative Golgi elements (Figure 3M), consistent with fluorescence microscopy. The anti-GFP gold-labeled tubules, which are labeled by HRP but not Tf-HRP, therefore represent GEECs. Together these data show that GEECs are distinct endosomal compartments and constitute a major pinocytic pathway in these cells.

Internalization into GEECs Is Specific and Requires GPI Anchoring

To determine whether the GPI anchor is required for delivery to GEECs, we examined the internalization of

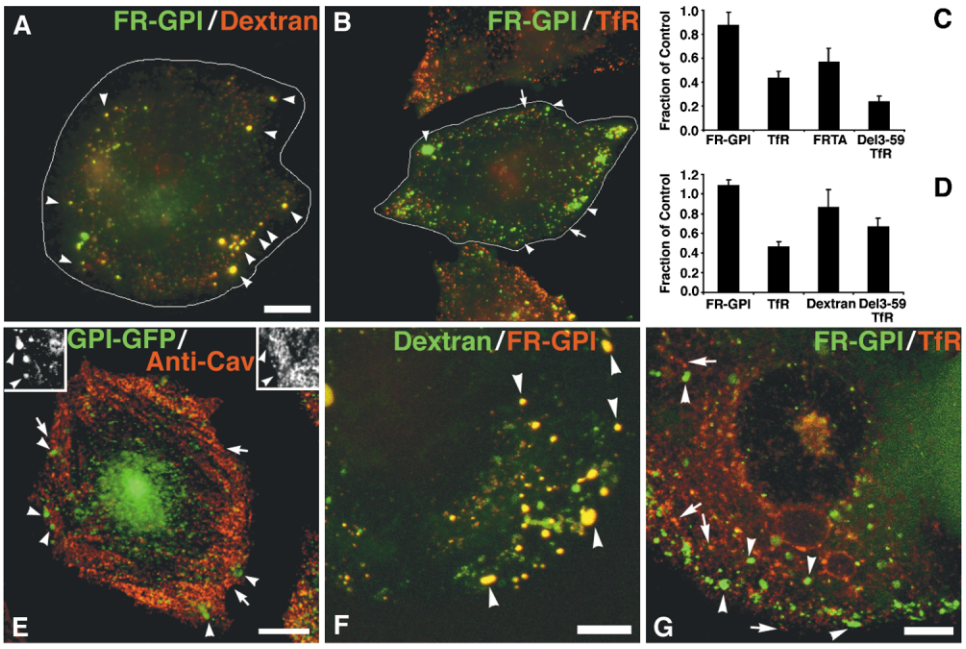

Figure 5. GPI-APs Are Endocytosed via Pinosomes Independent of Dynamin, Clathrin, and Caveolin Function

(A and B) FRαTb-1 cells transfected with GFPdyn2K44A (white outline) were labeled with Cy5-FabMOv19 and LR-Dex (A) or Alexa568-Tf (B) for 2 min at 37°C. GEECs (arrowheads) and Tf-containing sorting endosomes (arrows) remain distinct in the transfected cells.

(C and D) Histograms show extent of uptake expressed as fraction of that in control cells of indicated endocytic tracers in cells subjected to potassium depletion (C) or transfected with dyn2K44A (D). Values represented are mean ($\pm$SEM, receptor uptake; $\pm$SD, dextran uptake) obtained from at least two to five experiments each. Uptake of FR-GPI and Dextran was not statistically different from control cells (p values $>$ 0. 4), obtained from Student's t test by comparing the data sets from treated versus untreated cells.

(E) Intracellular GPI-GFP fluorescence (green) and caveolin 1 immunofluorescence (red) visualized using confocal microscopy in GG8Tb-1 cells treated with CHX is shown as color merges of a single confocal plane. Inset shows grayscale images of the area marked by an asterisk.

(F and G) CaCo-2 cells were incubated with Alexa568-FabMov18 and F-Dex (1 mg/ml; [F]) or Alexa488-FabMov18 and Alexa568-Tf (G) for 20 min at 37°C, and imaged live on a confocal microscope after removal of surface fluorescence. Arrowheads indicate the GEECs and arrows indicate the Tf-positive endosomes.

Bars, 10 μm.

two transmembrane isoforms of FR-GPI, FR-TM (Varma and Mayor, 1998), and FR-TA (Chatterjee et al., 2001). Unlike FR-GPI, $\sim$70% of FR-TM (Figure 4C) and FR-TA (Figures 4A and 4C) are colocalized with cointernalized Tf. Furthermore, FR-TM, FR-TA, and a tailless TfR lacking all except for three amino acids of the cytoplasmic tail (δ3-59TfR; McGraw and Maxfield, 1990) are all excluded from the F-Dex-filled tubular vesicular endosomes (data not shown). We have also examined the endocytic itinerary of exogenously introduced *N*-[*N*-(7-nitro-2,1,3-benzoxadiazol-4-yl)-ϵ-aminohexanoyl]-sphingosylphosphorylcholine (C_6-NBD-SM), which, similar to GPI-APs (Mayor et al., 1994), is diffusely distributed at the cell surface (Koval and Pagano, 1989). Quantitatively similar to FR-TM and FR-TA, C_6-NBD-SM, is extensively colocalized with TfR (Figure 4C) but not with FR-GPI after 2 min of internalization (Figures 4B and 4C). C_6-NBD-SM is also extensively colocalized with δ3-59TfR (Figure 4C). Furthermore, FR-TM, FR-TA, and C_6-NBD-SM remain colocalized with TfR throughout their endocytic pathway and accumulate in the RE with similar kinetics as TfR (Chatterjee et al., 2001; Mayor et al., 1993). In addition to FR-GPI and DAF, GPI anchoring of a signalless GFP moiety directs GFP to GEECs (Figure 1 and Supplemental Data, Figure S2 [http://www.developmentalcell.com/cgi/content/full/2/4/411/DC1]). These data conclusively show that internalization into GEECs is a specific process; neither the absence of clathrin pit sequestration potential (FR-TA; δ3-59TfR) nor the complete absence of a cytoplasmic tail (C_6-NBD-SM) is sufficient for inclusion of membrane components into this endocytic pathway.

GPI-APs Are Delivered to the RE via GEECs

To ascertain whether peripheral GEECs are involved in the direct delivery of the GPI-AP to the RE, we used a pulse-chase protocol (Figures 4D and 4E). Immediately after internalization (2 min), a majority ($\sim$70%) of FR-GPI is not colocalized with the peripheral TfR-containing sorting endosomes (Figures 2 and 4D), and following a 10 min chase at 37°C, most of the intracellular FR-GPI is colocalized with TfR in the RE (Figure 4E, open triangle, also see inset). No additional colocalization of FR-GPI with Tf-containing endosomes is observed even when Tf is maintained throughout the pulse chase period (data not shown). FR-GPI remains segregated from Tf in peripheral compartments even after a 20 min continuous pulse (Figure 4F, arrowheads). These observations show that FR-GPI traffics through distinct peripheral GEECs en route to the RE.

To investigate the mode of delivery of internalized GPI-APs to the RE from the GEECs, we labeled FRαTb-1

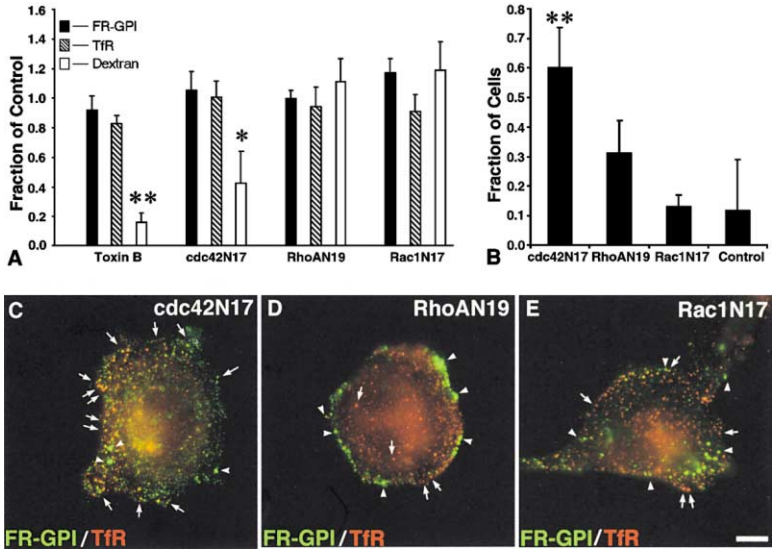

Figure 6. Rho Family GTPase cdc42 Regulates the Formation of GEECs

(A and B) Quantitative measurement of net endocytic uptake of FR-GPI (filled bar), TfR (hatched bar), in cells treated with toxin B or transfected with cdc42N17, RhoAN19, or Rac1N17 as indicated. Dextran uptake (empty bar) is represented as the fraction of cells showing a high level of uptake relative to untransfected (control) cells in each case. Histogram in (A) shows the uptake of each probe relative to that in untransfected cells in the same experiment. Data are mean (±SEM, receptor uptake; ±SD, dextran uptake) obtained from two to six experiments, each with ≥100 cells per experiment. Histogram in (B) shows fraction of cells with colocalization index between 0.4 and 1.0 (obtained as described in Figure 1F) between FR-GPI and TfR in FRαTb-1 cells transfected with cdc42N17, RhoAN19, or Rac1N17. Values are mean and standard deviation from two to five experiments. Double asterisks (**) or a single asterisk (*) denotes p values <0.004 and <0.04, respectively, obtained from Student's t test by comparing the data sets from treated versus untreated cells. Unmarked data sets are not significantly different from control cells ($p > 0.6$).

(C–E) Pseudocolored images depicting the extent of colocalization between FR-GPI (green) and TfR (red) in cells transfected with cdc42N17 (C), RhoAN19 (D), and Rac1N17 (E). Arrowheads indicate GEECs; arrows indicate Tf-filled sorting endosomes.

Bar, 10 μm.

cells with fluorescent ligands for TfR and FR-GPI and imaged living cells. Many FR-GPI-containing GEECs continuously extend tubules, some of which detach and are propelled inwards to fuse with the RE (see movie in Supplemental Data [http://www.developmentalcell.com/cgi/content/full/2/4/411/DC1]). These GEECs, thereby, seem to empty their membrane cargo into the RE, resulting in the lumenal and morphological colocalization observed between multiple GPI-APs and TfR (Mayor et al., 1998; see Supplemental Data, Figure S2 [http://www.developmentalcell.com/cgi/content/full/2/4/411/DC1]).

GPI-APs Are Internalized into GEECs via a Clathrin Pit- and Caveolae-Independent Pathway

To determine whether clathrin function is involved in the internalization of GPI-APs, we either depleted cells of potassium to disrupt the formation of clathrin-coated pits (Larkin et al., 1983) or, by the expression of a dominant-negative isoform of dyn2 (dyn2K44A; Cao et al., 1998), inhibited their pinching off (McNiven et al., 2000). Expression of dyn2K44A or K^+ depletion did not affect the uptake of Lissamine Rhodamine-conjugated Dex (LR-Dex) and FR-GPI, qualitatively (Figures 5A and 5B, arrowheads) or quantitatively (Figures 5C and 5D). On the other hand, endocytosis of TfR, δ3-59TfR, and FR-TA was significantly inhibited (Figures 5C and 5D). In separate experiments, expression of a dominant-negative isoform of eps15 (EΔ95/295; Benmerah et al., 2000) also inhibited TfR endocytosis to the same extent as dynK44A expression, but did not affect FR-GPI or Dextran uptake (data not shown). These results show that the formation of GEECs is independent of clathrin and dyn2 function.

To ascertain whether GEECs are formed via caveolin-coated intermediates, we analyzed the distribution of caveolin on GEECs by immunofluorescence microscopy, since endocytosis via caveolae results in structures that retain the caveolin coat (Pelkmans et al., 2001; Puri et al., 2001). Caveolin is detected in punctate arrays on the plasma membrane but is not present on the peripheral GPI-GFP-containing GEECs (Figure 5E, arrowheads; see insets) or compartments containing FR-GPI in FRαTb-1 cells expressing caveolin 1-GFP (Supplemental Data [http://www.developmentalcell.com/cgi/content/full/2/4/411/DC1]), suggesting that caveolin is not involved in this process of endocytosis. To confirm that caveolae are not necessary for the formation of GEECs, we examined the endocytic pathway of endogenously expressed FR-GPI in CaCo-2 cells, which do not have morphologically identifiable caveolae or express caveolin 1 and 2 (Vogel et al., 1998). The distribution of internalized FR-GPI in CaCo-2 cells is similar in all respects to that observed in the caveolin-containing cell types; FR-GPI is cointernalized with F-Dex into GEECs, which are devoid of cointernalized TfR (Figures 5F and 5G, arrowheads). Together, these data strongly suggest that the uptake of GPI-APs and fluid-phase via GEECs is independent of caveolin or clathrin coats and dyn function.

Fluid-Phase and GPI-AP Uptake into GEECs Are Modulated by cdc42

Recently Rho family GTPases have been shown to play a regulatory role in endocytic processes (Ellis and Mellor, 2000). To examine whether these GTPases regulate the formation of GEECs, we used *Clostridium difficile* toxin, toxin B, which irreversibly inactivates the Rho family GTPases by glucosylation (Aktories et al., 2000). Toxin B treatment caused a general alteration of cell morphology and actin organization as described previously (Just et al., 1994) and inhibited the endocytosis of the fluid-phase markers without affecting the internalization of

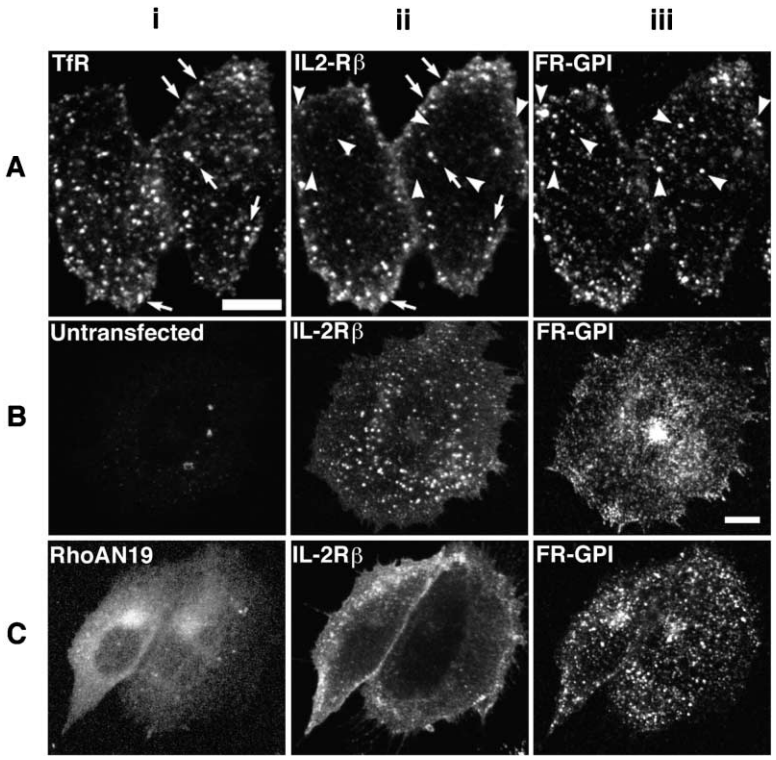

Figure 7. DRM-Associated IL2-Rβ Is Not Internalized into GEECs

FR-GPI-expressing CHO cells transiently transfected with IL2-Rβ were incubated with Alexa568-mAb561 (ii), and Cy5-FabMov19 (iii) for 5 min (A) or 15 min (B and C) at 37°C. In (A), cells were incubated with Og-Tf (i). (B) (i) and (C) (i) show the absence (B) or presence (C) of *myc*-RhoAN19 expression as detected by FITC-anti-*myc* fluorescence in cells cotransfected with IL2-Rβ and *myc*-RhoAN19. Arrowheads indicate GEECs; arrows indicate Tf-filled sorting endosomes.
Bar, 10 μm.

FR-GPI or TfR (Figure 6A), suggesting a role for Rho family GTPases in fluid-phase endocytosis. To dissect the effects of inactivation of individual Rho family GTPases, we expressed dominant-negative isoforms of RhoA, Rac1, and cdc42. In cells expressing equivalent levels of *myc*-tagged isoforms of cdc42N17, RhoAN19, or Rac1N17, or GFP-tagged isoforms of cdc42N17 or Rac1N17, only the cdc42N17 isoform dramatically reduced the fraction of cells showing a high uptake of dextran without affecting Tf internalization (Figure 6A). Expression of *myc*-RhoAN19 inhibited IL2-Rβ internalization in the same cells (Figure 7). Furthermore, compared to control cells, dextran uptake is quantitatively reduced in toxin B-treated or cdc42N17-expressing cells to 32% ± 4% or 64% ± 11%, respectively. Net dextran uptake was relatively unaffected in RhoAN19 (105% ± 24%) or Rac1N17-transfected cells (130% ± 22%). The reproducible reduction of fluid-phase internalization in cdc42N17 (but not in RhoAN19 and Rac1N17) expressing cells seems to be due to the reduced size of GEECs (Figure 6C); higher cdc42N17-expressing cells show fewer GEECs.

The lack of a detectable effect on the net internalization of GPI-APs in either toxin B-treated or cdc42N17-expressing cells (Figure 6A) was surprising and suggests that GPI-APs may also be internalized by another pathway. To examine whether GPI-APs are now internalized mainly via sorting endosomes, we determined the extent of colocalization of FR-GPI and Tf at early times in cells expressing dominant-negative Rho family GTPase isoforms. Toxin-B treatment significantly altered the morphology of cells, precluding analysis of colocalization by wide-field microscopy. In cells expressing cdc42N17, the extent of colocalization of GPI-APs and TfR was clearly increased (Figure 6C); ~60% of transfected cells showed a high degree of colocalization (range 40%–80%) with TfR (Figures 6B and 6C). Expression of RhoAN19 and Rac1N17 caused no change in the extent of colocalization of FR-GPI and TfR with respect to untransfected cells (Figures 6B, 6D, and 6E).

Expression of dominant-active isoform of cdc42 (GFP-cdc42L61) has no effect on the extent of formation of GEECs as assessed by the lack of perturbation of fluid-phase uptake and the extent of colocalization of GPI-APs and TfR at early times (data not shown). On the other hand, expression of dominant-active GFP-Rac1L61 at the same levels resulted in an increase in fluid-phase uptake consistent with the formation of very large macropinocytic structures (~3–6 μm diameter phase lucent structures) distinct from the GEECs (Dharmawardhane et al., 2000) containing both TfR and GPI-APs (data not shown). The net uptake of Tf in GFP-Rac1L61-expressing cells was reduced to 40% (±7%) of that in untransfected cells, consistent with previous studies (Lamaze et al., 1996). Together, these data show that inactivation of a specific Rho family GTPase, cdc42, inhibits the clathrin-independent GEEC pathway, resulting in the redirection of GPI-APs toward the clathrin-dependent pathway.

DRM-Associated IL2R Is Not Internalized via GEECs

Since both IL2-Rβ (Lamaze et al., 2001) and GPI-APs (Mayor and Maxfield, 1995) are present in DRMs at the cell surface, we determined whether IL2-R and FR-GPI are internalized into the same endosomes. For this purpose, we have visualized the endocytic pathway of coexpressed IL2-Rβ and FR-GPI in CHO cells, using

exogenously added fluorescently labeled antibodies. In the same cells, while IL2-Rβ and FR-GPI are both present in DRMs (assayed as described previously; Lamaze et al., 2001), IL2-Rβ is not detected in FR-GPI-containing GEECs (Figure 7A, arrowheads). However, IL2-Rβ is internalized into endosomes that contain the transferrin receptor at these times (Figure 7A, arrows), consistent with previous studies (Hemar et al., 1995). At later times (>15 min), IL2-Rβ is mainly detected in late endosomes (Hemar et al., 1995), devoid of TfR (data not shown) and FR-GPI (Figure 7B). Expression of RhoAN19 inhibits the internalization of IL2-Rβ; however, the formation of GEECs containing FR-GPI is unaffected in the same cells (Figure 7C). These data show that, although FR-GPI and IL2-Rβ are both in DRMs, they are internalized via different pathways and mechanisms.

Discussion

In this report, we provide evidence that GPI-APs are selectively recruited to a cdc42-regulated, clathrin- and caveolin-independent pinocytic pathway composed of acidic endosomes that we term GEECs. GPI-APs are then directly delivered, often via tubular intermediates, to the RE. These studies have revealed a parallel rab5-independent endocytic pathway for the selective internalization of GPI-APs as schematized in the model in Figure 8. Consistent with previous observations (Chatterjee et al., 2001; Mayor et al., 1998), these results confirm that multiple GPI-APs are recycled to the PM via the RE; endocytosed GPI-APs are not delivered to the Golgi. This contrasts with a recent report from Nichols et al. (2001).

The characteristic 28–40 nm GPI-AP and fluid-filled peripheral tubular vesicular elements, negative for the presence of markers of the clathrin-mediated pathway and rab proteins (rab 4, 5, and 7), represent distinct early endosomal elements of this pathway. Previous attempts at characterizing the fluid-phase pathway using the tracer, HRP, revealed a tubular early endosomal network at the periphery of cells and also tubular elements at the pericentriolar region (Tooze and Hollinshead, 1991). While these studies did not suggest a parallel endocytic pathway of membrane components to the RE, they are consistent with the proposed model. The discovery of this pathway also explains the segregation of a fraction (~30%) of the internalized FR-GPI and DAF pool from TfR as measured by HRP-mediated quenching and immuno-EM methodologies, respectively (Mayor et al., 1998). This segregation is quantitatively consistent with the measured rates of exit from the GEECs and accumulation in the RE ($t_{1/2}$ ~12 min and ~30 min, respectively; Chatterjee et al., 2001).

The GPI anchor appears to be a positive signal for the recruitment of membrane proteins to the GEECs. Native GPI-APs (FR-GPI, DAF) or a chimeric GPI-AP (GPI-GFP) are included in GEECs, whereas proteins wherein the GPI anchor has been replaced with a transmembrane tail (FR-TM or FR-TA) or molecules without cytoplasmic extensions (δ3-59TfR, C_6-NBD-SM) are all excluded (Figure 4). Although the role of the GPI anchor as a sorting determinant for targeting proteins to the apical surface in polarized epithelia has been recently

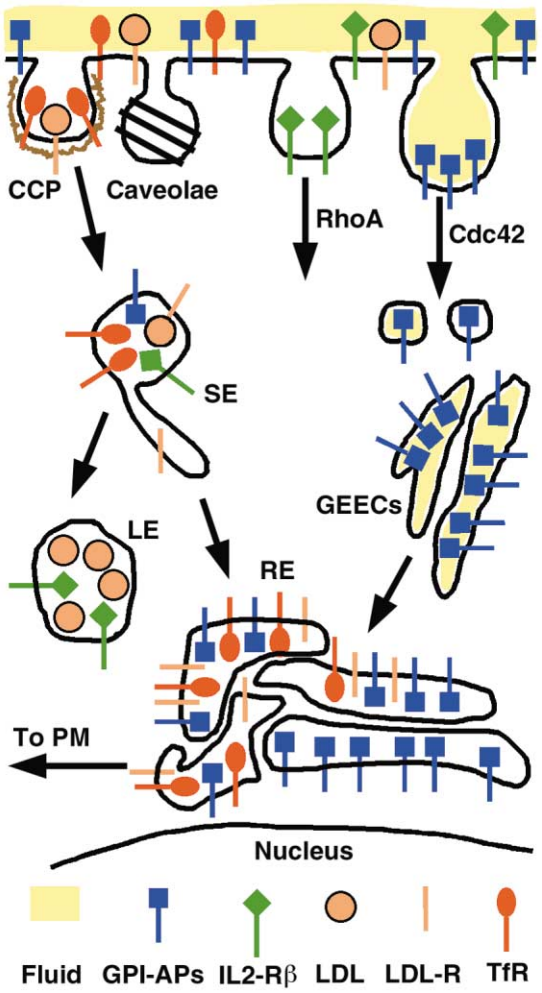

Figure 8. Schematic of the GPI-AP Endocytic Pathway

Cell surface molecules are internalized via dynamin-independent (GPI-AP), and dynamin-dependent pathways that include clathrin-coated pit (CCP), caveolae, and the RhoA-dependent mechanisms. In the case of the CCP-mediated pathway, molecules traffic from sorting endosomes (SE) to the recycling endosomal compartment (RE) and/or late endosomes (LE). Receptors and other membrane components in the RE are returned to the plasma membrane, whereas molecules in late endosomes are subsequently degraded in the lysosomes. GPI-APs and fluid phase are internalized via endocytic vesicles distinct from caveolin and clathrin-coated vesicles, into tubular-vesicular endosomes called GEECs, in a cdc42-regulated fashion. GPI-APs are subsequently trafficked to the cell-surface (PM) via perinuclear RE but not the Golgi.

questioned (Benting et al., 1999; Lipardi et al., 2000), these results indicate that the GPI anchor is *necessary* for the sorting of membrane proteins to GEECs.

The sorting of GPI-APs toward GEECs is likely to occur at the cell surface for the following reasons. First, perturbants of the function of dyn and clathrin, molecules involved in forming vesicles at the cell surface (McNiven, 1998), do not inhibit the endocytosis of GPI-APs or the fluid-phase. They inhibit the endocytosis of proteins containing or lacking clathrin localization motifs (Figure 5) or molecules completely lacking cytoplasmic extensions including exogenously introduced fluorescent lipids (Hao and Maxfield, 2000; Puri et al., 2001), suggesting

that dyn- and clathrin-dependent pathways accommodate membrane molecules in a more permissive fashion. Second, GPI-APs are detected in separate fluid-filled endosomes and small vesicles at very early times (~1–2 min), often in distinct regions of the cell (Figure 4). At these times, markers of the clathrin-dependent pathway are present at close to steady-state levels in sorting endosomes ($t_{1/2}$ ~2 min; Hao and Maxfield, 2000; Mayor et al., 1993). Finally, cdc42 selectively modulates the extent of endocytosis via GEECs but does not affect endocytosis of TfR (Figure 6).

Internalization of GPI-APs into GEECs represents a distinct type of clathrin-independent endocytic mechanism. It is clearly different from that of DRM-associated IL2-R (Lamaze et al., 2001); IL2-R internalization is blocked by expression of dominant-negative RhoA (Lamaze et al., 2001), whereas GPI-AP and fluid-phase uptake are unaffected (Figures 6 and 7). Furthermore, inhibition of the activity of dyn isoforms does not affect GEEC formation. Neither GPI-AP nor fluid-phase uptake (dyn2 aa; Figure 5), or intoxication via *Diptheria* toxin (dyn1 aa; Skretting et al., 1999) and *Helicobacter pylori* Vac A toxin (dyn2 ba; Ricci et al., 2000) internalized via GPI-anchored receptors, is affected by inhibition of dyn isoform activity. On the other hand, internalization of IL2-R (Lamaze et al., 2001) and BODIPY-labeled sphingolipids (Puri et al., 2001) rely on dyn-dependent mechanisms. The GEEC pathway is unlike the caveolar endocytic pathway that facilitates SV40 virus entry into CV-1 cells via "caveosomes" derived from surface caveolae. Caveosomes are neutral pH compartments outlined by caveolin, and do not cointernalize fluid-phase markers (Pelkmans et al., 2001). Finally, GPI-AP and fluid-phase uptake via GEECs appears distinct from other means of fluid-phase endocytosis such as stimulated macropinocytosis (Hewlett et al., 1994) or developmentally regulated pinocytosis in maturing dendritic cells (Garrett et al., 2000; West et al., 2000). Unlike the case with GEECs, inhibition of Rac1 activity completely blocks fluid uptake via these pathways (Dharmawardhane et al., 2000; Garrett et al., 2000; West et al., 2000). In addition, macropinosomes are large phase-lucent structures easily visualized in bright-field microscopy, while GEECs do not appear to have phase-lucent counterparts. Thus, the GEEC pathway is a distinct constitutive pinocytic process, responsible for a majority of fluid-phase uptake in CHO cells.

The selective recruitment of GPI-APs to this endocytic pathway may be related to the ability of GPI-APs to associate with cholesterol and sphingolipid-enriched rafts since GPI-APs occur as cholesterol-dependent submicron-sized domains at the cell surface (Friedrichson and Kurzchalia, 1998; Pralle et al., 2000; Varma and Mayor, 1998). Consistent with this, preliminary experiments show that cholesterol depletion selectively reduces the formation of GEECs (Sabharanjak et al., unpublished data). However, the ability of IL2-R to partition into DRMs is clearly not sufficient to allow its inclusion into GEECs, suggesting that DRMs may consist of different types of endocytically active units capable of being segregated at the cell surface.

The recognition of a role of the Rho family GTPases in endocytosis indicates regulatory control of actin polymerization (Ellis and Mellor, 2000). It is thus intriguing that cdc42 (but not other Rho family GTPases) is involved in this pathway. Cdc42 is a key regulator of N-WASP, known to stimulate the actin-nucleating Arp2/3 complex, by directly binding to N-WASP and uncoupling the inhibitory activity of its N-terminal domain (Rohatgi et al., 2000). Further experiments will help elucidate a mechanism involving cdc42 and its effectors in this endocytic process.

The discovery of the GPI anchor as a specific sorting determinant for internalization via this cdc42-regulated, nonclathrin and caveolae-independent, pinocytic pathway will aid in identifying other cell surface constituents and understanding the molecular mechanisms of this constitutive endocytic process. Since it mediates uptake of a significant fraction of the fluid phase and is selective for GPI-Aps, this pathway is likely to be of considerable biological and immunological significance. In addition, folate uptake via the folate receptor (Ritter et al., 1995) and scrapie formation from PrP^C (Kaneko et al., 1997; Taraboulos et al., 1995) may be greatly facilitated by their ability to be targeted to GEECs.

Experimental Procedures

Materials

All chemicals and reagents were from Sigma Chemical Co. (St. Louis, MO), and fluorescent reagents and probes from Molecular Probes (Eugene, OR), or as described earlier (Chatterjee et al., 2001; Mayor et al., 1998), unless otherwise specified. LDL was prepared from fetal bovine serum as described (Mayor et al., 1993). Cy5 labeling reagent was obtained from Amersham Pharmacia Biotech (UK). *Clostridium difficile* toxin B was a gift from Dr. Patrice Bouquet (Institut National de la Sante et de la Recherche Medicale, Nice, France).

cDNA, Antibodies, and Cell Culture

All plasmids, antibodies, and cell lines are described in Tables 1–3 in Supplemental Data [http://www.developmentalcell.com/cgi/content/full/2/4/411/DC1].

Cell Labeling and Other Treatments

Cells were incubated with appropriate combinations of the endocytic tracers for the indicated times in labeling medium (f-HF-12, 5% dialyzed serum). F-Dex, LR-Dex (1 mg/ml), or Lucifer yellow was used to mark the fluid phase. Fluorescently labeled Fab fragments (4 μg/ml) of MOv18, MOv19, or folate receptor ligands (30 nM), PLF and PLR (FR isoforms), IA10 (5 μg/ml) (DAF), Tf (10 μg/ml), were obtained as described previously (Chatterjee et al., 2001; Mayor et al., 1998) and used at the indicated concentrations. CTxB was labeled with Cy3 according to the manufacturer's instructions and incubated with cells at 1 μg/ml for indicated times. GFP-expressing GG8Tb-1 cells were labeled with purified anti-GFP mAb, (1B3A8; 4 μg/ml) on ice for 45 min, washed and incubated at 37°C for 1 hr. Fluorescently labeled anti-GFP antibodies (Fl-anti-GFP) are not dissociated from GFP by extended exposure at the cell surface to low pH (pH 4.6) buffers, nor released into a soluble pool in the lumen of endosomes (data not shown), confirming the use of Fl-anti-GFP as a marker for following endocytosis of GFP-tagged proteins. All labeled primary and secondary antibodies (and their fragments) were tested for their specific binding to their respective antigens by ensuring that cells which did not express these antigens showed undetectable labeling. Specificity of the labeled ligands was similarly confirmed in the presence of excess unlabeled competitors.

After incubation with labeled tracers, excess label was washed off with medium 1 (Mayor et al., 1998). To visualize the endosomal distribution of the fluorescent tracers, cells were cooled on ice and the cell-surface label (fluorescently labeled Tf, PLF, or PLR) was removed by incubating cells in ice-cold ascorbate buffer pH 4.5 (160 mM sodium ascorbate, 40 mM ascorbic acid, 1 mM $MgCl_2$, 1

mM $CaCl_2$) for 30 min; surface fluorescence from labeled Fab fragments or intact antibody against GPI-APs was removed by PI-PLC treatment. To visualize C_6-NBD-SM-labeled endosomes, surface-incorporated C_6-NBD-SM (Mukherjee et al., 1999) was back exchanged after 2 min incubation at 37°C and imaged exactly as described (Mayor et al., 1993).

Cycloheximide was used to inhibit protein synthesis and remove contribution from biosynthetic traffic in CHO (50 μg/ml; 3 hr at 37°C) and Cos-7 cells (200 μg/ml; 4–5 hr at 37°C).

For visualizing endosomal compartments in living cells, labeled cells were directly taken for imaging after incubation with PI-PLC (10 U/ml) for 2 min at room temperature to remove surface GPI-AP-associated fluorescence. In all other experiments, endosomal pH was neutralized by incubation in nigericin (10 μM) in a high-potassium buffer (120 mM KCl, 1 mM $MgCl_2$, 1 mM $CaCl_2$, 20 mM HEPES, pH 7.2). Cells were depleted of potassium prior to labeling with endocytic tracers as described (Larkin et al., 1983). Cells were transiently transfected using Fugene6 according to the manufacturer's instructions (Roche Molecular Biochemicals). Transfected cells were identified by GFP fluorescence or by immunostaining of the epitope-tagged proteins expressed in the cell using appropriate anti-epitope antibodies.

Immunofluorescence Microscopy

For immunostaining cells were fixed and permeabilized using different protocols as described in Supplemental Data (http://www.developmentalcell.com/cgi/content/full/2/4/411/DC1). These protocols were necessary to visualize the true extent of endosomal distributions of GPI-APs since standard fixation and permeabilization conditions quantitatively and qualitatively disrupted GPI-AP distribution.

Electron Microscopy

After transfection with GPI-GFP for 24 hr, CHO cells were incubated with anti-GFP-gold plus 10 mg/ml HRP. Alternatively, cells were incubated with 50 μg/ml Tf-HRP (Pierce). They were then incubated for various times before fixation and processing for HRP visualization and upon embedding as described previously (Parton et al., 1994). Transfected cells were readily recognized by their high GPI-GFP-gold labeling; untransfected cells showed negligible labeling. Fifty and 200 nm sections were viewed unstained. The validity of the anti-GFP-gold labeling scheme to track the GPI-anchored proteins was assessed in parallel by immunofluorescence (data not shown).

Endocytic Uptake Assays

For quantitative measurements of the fluid phase, cells were incubated with fluorescently conjugated dextran for 5 or 20 min and washed extensively prior to imaging. Endocytic uptake of all probes was quantified at low magnification (20×) as described (Chatterjee et al., 2001).

Imaging and Image Processing

Confocal imaging was carried out on a Bio-Rad MRC 1024 confocal microscope (Bio-Rad Microsciences, UK) equipped with factory set dichroics and an Argon-Krypton laser. To image processes in living cells, confocal images were captured using time course acquisition software (Bio-Rad). Images were acquired and corrected for crosstalk as described in Supplemental Data (http://www.developmentalcell.com/cgi/content/full/2/4/411/DC1). High-resolution wide-field images were collected using Nikon TE 300 or Nikon TMD inverted microscope equipped with 60×, 1.4 NA and 20×, 0.75 NA objectives, a mercury arc illuminator (Nikon, Japan), and a cooled CCD camera (Princeton Instruments, NY) controlled by Metamorph software (Universal Imaging, PA). Optimized dichroics, excitation, and emission filters were used as described (Chatterjee et al., 2001). Images collected on the wide field showed no detectable crosstalk between the different fluorophores.

The quantification of colocalization of endocytic markers in high-resolution wide-field images was determined using established software routines capable of identifying and quantifying the intensity of each endosomes, followed by determining the extent of colocalization of individual endosomes with identified endosomes in a reference image (see Supplemental Data [http://www.developmentalcell.com/cgi/content/full/2/4/411/DC1]). The colocalization index was calculated as a ratio of the colocalized intensity to the total intensity of the probe in endosomes identified in each cell. The colocalization index is represented as a mean and standard error of the mean obtained from two to five independent experiments with a minimum of 30 cells per experiment. Maximum extent of colocalization obtained by this method is 80% for the colocalization of cointernalized Alexa568-Tf and Cy5-Tf in the same cell. Detailed procedures are provided in Supplemental Data (http://www.developmentalcell.com/cgi/content/full/2/4/411/DC1).

All images were processed for output purposes using Adobe Photoshop software.

Acknowledgments

We are extremely grateful to Chas Ferguson and Amanda Carozzi for assistance with electron microscopic experiments and Neha Vyas for purifying the plasmids. We would like to thank to S. Canaveri and Centecor Corp. for their generous gift of FR antibodies; D. Brown and M. Low for *B. thuringiensis* PI-PLC; C. Zurzolo, E. Rodriguez-Boulan, M. Way, M. Zerial, A. Yap, M. McNiven, B. Nichols, R. Lodge, L. Pelkmans, and J. Lippincott-Schwartz for cDNAs used; R. Vishwakarma for folic acid analogs; S. Sunderesan for anti-GFP monoclonal; T. Kurzchalia for GFP-Cav-1 cells; U. Tatu for ER antiserum and Cos-7 cells; I. Prior for anti-GFP-gold; the National Centre for Cell Science; Pune for providing several cell lines; R. Varma, V. Sriram, and R. Chadda for critically reading this manuscript; and other members of the Mayor laboratory for help. This work was in part supported by a Senior Research Fellowship to S.M. from The Wellcome Trust (grant 056727/Z/99) and funds from The Mizutani Foundation and the National Centre for Biological Sciences. S.S. and P.S. are recipients of the Kanwal Rekhi fellowship from the TIFR Endowment Fund. S.S would like to thank Avinash Shenoy and all her family for encouragement. S.M. thanks F.F. Bosphorus and K. Belur for inspiration.

Received: October 9, 2001
Revised: March 20, 2002

References

Aktories, K., Schmidt, G., and Just, I. (2000). Rho GTPases as targets of bacterial protein toxins. Biol. Chem. *381*, 421–426.

Anderson, R.G., Kamen, B.A., Rothberg, K.G., and Lacey, S.W. (1992). Potocytosis: sequestration and transport of small molecules by caveolae. Science *255*, 410–411.

Benmerah, A., Poupon, V., Cerf-Bensussan, N., and Dautry-Varsat, A. (2000). Mapping of Eps15 domains involved in its targeting to clathrin-coated pits. J. Biol. Chem. *275*, 3288–3295.

Benting, J.H., Rietveld, A.G., and Simons, K. (1999). N-Glycans mediate the apical sorting of a GPI-anchored, raft-associated protein in Madin-Darby canine kidney cells. J. Cell Biol. *146*, 313–320.

Bergelson, J.M., Chan, M., Solomon, K.R., St John, N.F., Lin, H., and Finberg, R.W. (1994). Decay-accelerating factor (CD55), a glycosylphosphatidylinositol-anchored complement regulatory protein, is a receptor for several echoviruses. Proc. Natl. Acad. Sci. USA *91*, 6245–6249.

Borchelt, D.R., Taraboulos, A., and Prusiner, S.B. (1992). Evidence for synthesis of scrapie prion proteins in the endocytic pathway. J. Biol. Chem. *267*, 16188–16199.

Cao, H., Garcia, F., and McNiven, M.A. (1998). Differential distribution of dynamin isoforms in mammalian cells. Mol. Biol. Cell *9*, 2595–2609.

Chan, S.Y., Empig, C.J., Welte, F.J., Speck, R.F., Schmaljohn, A., Kreisberg, J.F., and Goldsmith, M.A. (2001). Folate receptor-alpha is a cofactor for cellular entry by Marburg and Ebola viruses. Cell *106*, 117–126.

Chatterjee, S., and Mayor, S. (2001). The GPI-anchor and protein sorting. Cell. Mol. Life Sci. *58*, 1967–1987.

Chatterjee, S., Smith, E.R., Hanada, K., Stevens, V.L., and Mayor, S. (2001). GPI anchoring leads to sphingolipid-dependent retention of endocytosed proteins in the recycling endosomal compartment. EMBO J. *20*, 1583–1592.

Dharmawardhane, S., Schurmann, A., Sells, M.A., Chernoff, J., Schmid, S.L., and Bokoch, G.M. (2000). Regulation of macropinocytosis by p21-activated kinase-1. Mol. Biol. Cell *11*, 3341–3352.

Diep, D.B., Nelson, K.L., Raja, S.M., Pleshak, E.N., and Buckley, J.T. (1998). Glycosylphosphatidylinositol anchors of membrane glycoproteins are binding determinants for the channel-forming toxin aerolysin. J. Biol. Chem. *273*, 2355–2360.

Dunn, K.W., McGraw, T.E., and Maxfield, F.R. (1989). Iterative fractionation of recycling receptors from lysosomally destined ligands in an early sorting endosome. J. Cell Biol. *109*, 3303–3314.

Ellis, S., and Mellor, H. (2000). Regulation of endocytic traffic by rho family GTPases. Trends Cell Biol. *10*, 85–88.

Ferguson, M.A. (1999). The structure, biosynthesis and functions of glycosylphosphatidylinositol anchors, and the contributions of trypanosome research. J. Cell Sci. *112*, 2799–2809.

Friedrichson, T., and Kurzchalia, T.V. (1998). Microdomains of GPI-anchored proteins in living cells revealed by crosslinking. Nature *394*, 802–805.

Fujimoto, T. (1996). GPI-anchored proteins, glycosphingolipids, and sphingomyelin are sequestered to caveolae only after crosslinking. J. Histochem. Cytochem. *44*, 929–941.

Garrett, W.S., Chen, L.M., Kroschewski, R., Ebersold, M., Turley, S., Trombetta, S., Galan, J.E., and Mellman, I. (2000). Developmental control of endocytosis in dendritic cells by Cdc42. Cell *102*, 325–334.

Hao, M., and Maxfield, F.R. (2000). Characterization of rapid membrane internalization and recycling. J. Biol. Chem. *275*, 15279–15286.

Hemar, A., Subtil, A., Lieb, M., Morelon, E., Hellio, R., and Dautry-Varsat, A. (1995). Endocytosis of interleukin 2 receptors in human T lymphocytes: distinct intracellular localization and fate of the receptor alpha, beta, and gamma chains. J. Cell Biol. *129*, 55–64.

Hewlett, L.J., Prescott, A.R., and Watts, C. (1994). The coated pit and macropinocytic pathways serve distinct endosome populations. J. Cell Biol. *124*, 689–703.

Just, I., Richter, H.P., Prepens, U., von Eichel-Streiber, C., and Aktories, K. (1994). Probing the action of Clostridium difficile toxin B in Xenopus laevis oocytes. J. Cell Sci. *107*, 1653–1659.

Kamen, B.A., Smith, A.K., and Anderson, R.G. (1991). The folate receptor works in tandem with a probenecid-sensitive carrier in MA104 cells in vitro. J. Clin. Invest. *87*, 1442–1449.

Kaneko, K., Vey, M., Scott, M., Pilkuhn, S., Cohen, F.E., and Prusiner, S.B. (1997). COOH-terminal sequence of the cellular prion protein directs subcellular trafficking and controls conversion into the scrapie isoform. Proc. Natl. Acad. Sci. USA *94*, 2333–2338.

Koval, M., and Pagano, R.E. (1989). Lipid recycling between the plasma membrane and intracellular compartments: transport and metabolism of fluorescent sphingomyelin analogues in cultured fibroblasts. J. Cell Biol. *108*, 2169–2181.

Lamaze, C., and Schmid, S.L. (1995). The emergence of clathrin-independent pinocytic pathways. Curr. Opin. Cell Biol. *7*, 573–580.

Lamaze, C., Chuang, T.H., Terlecky, L.J., Bokoch, G.M., and Schmid, S.L. (1996). Regulation of receptor-mediated endocytosis by Rho and Rac. Nature *382*, 177–179.

Lamaze, C., Dujeancourt, A., Baba, T., Lo, C.G., Benmerah, A., and Dautry-Varsat, A. (2001). Interleukin 2 Receptors and Detergent-Resistant Membrane Domains Define a Clathrin-Independent Endocytic Pathway. Mol. Cell *7*, 661–671.

Larkin, J.M., Brown, M.S., Goldstein, J.L., and Anderson, R.G. (1983). Depletion of intracellular potassium arrests coated pit formation and receptor-mediated endocytosis in fibroblasts. Cell *33*, 273–285.

Lipardi, C., Nitsch, L., and Zurzolo, C. (2000). Detergent-insoluble GPI-anchored proteins are apically sorted in fischer rat thyroid cells, but interference with cholesterol or sphingolipids differentially affects detergent insolubility and apical sorting. Mol. Biol. Cell *11*, 531–542.

Mayor, S., and Maxfield, F.R. (1995). Insolubility and redistribution of GPI-anchored proteins at the cell surface after detergent treatment. Mol. Biol. Cell *6*, 929–944.

Mayor, S., Presley, J.F., and Maxfield, F.R. (1993). Sorting of membrane components from endosomes and subsequent recycling to the cell surface occurs by a bulk flow process. J. Cell Biol. *121*, 1257–1269.

Mayor, S., Rothberg, K.G., and Maxfield, F.R. (1994). Sequestration of GPI-anchored proteins in caveolae triggered by cross-linking. Science *264*, 1948–1951.

Mayor, S., Sabharanjak, S., and Maxfield, F.R. (1998). Cholesterol-dependent retention of GPI-anchored proteins in endosomes. EMBO J. *17*, 4626–4638.

McGraw, T.E., and Maxfield, F.R. (1990). Human transferrin receptor internalization is partially dependent upon an aromatic amino acid on the cytoplasmic domain. Cell Regul. *1*, 369–377.

McNiven, M.A. (1998). Dynamin: a molecular motor with pinchase action. Cell *94*, 151–154.

McNiven, M.A., Cao, H., Pitts, K.R., and Yoon, Y. (2000). The dynamin family of mechanoenzymes: pinching in new places. Trends Biochem. Sci. *25*, 115–120.

Mukherjee, S., Ghosh, R.G., and Maxfield, F.R. (1997). Endocytosis. Physiol. Rev. *77*, 759–803.

Mukherjee, S., Soe, T.T., and Maxfield, F.R. (1999). Endocytic sorting of lipid analogues differing solely in the chemistry of their hydrophobic tails. J. Cell Biol. *144*, 1271–1284.

Nichols, B.J., Kenworthy, A.K., Polishchuk, R.S., Lodge, R., Roberts, T.H., Hirschberg, K., Phair, R.D., and Lippincott-Schwartz, J. (2001). Rapid cycling of lipid raft markers between the cell surface and Golgi complex. J. Cell Biol. *153*, 529–541.

Ohkuma, S., and Poole, B. (1978). Fluorescence probe measurement of the intralysosomal pH in living cells and the perturbation of pH by various agents. Proc. Natl. Acad. Sci. USA *75*, 3327–3331.

Parton, R.G., Joggerst, B., and Simons, K. (1994). Regulated internalization of caveolae. J. Cell Biol. *127*, 1199–1215.

Pelkmans, L., Kartenbeck, J., and Helenius, A. (2001). Caveolar endocytosis of simian virus 40 reveals a new two-step vesicular-transport pathway to the ER. Nat. Cell Biol. *3*, 473–483.

Pralle, A., Keller, P., Florin, E.L., Simons, K., and Horber, J.K. (2000). Sphingolipid-cholesterol rafts diffuse as small entities in the plasma membrane of mammalian cells. J. Cell Biol. *148*, 997–1008.

Puri, V., Watanabe, R., Singh, R.D., Dominguez, M., Brown, J.C., Wheatley, C.L., Marks, D.L., and Pagano, R.E. (2001). Clathrin-dependent and -independent internalization of plasma membrane sphingolipids initiates two Golgi targeting pathways. J. Cell Biol. *154*, 535–548.

Ricci, V., Galmiche, A., Doye, A., Necchi, V., Solcia, E., and Boquet, P. (2000). High cell sensitivity to Helicobacter pylori VacA toxin depends on a GPI-anchored protein and is not blocked by inhibition of the clathrin-mediated pathway of endocytosis. Mol. Biol. Cell *11*, 3897–3909.

Rijnboutt, S., Jansen, G., Posthuma, G., Hynes, J.B., Schornagel, J.H., and Strous, G.J. (1996). Endocytosis of GPI-linked membrane folate receptor-alpha. J. Cell Biol. *132*, 35–47.

Ritter, T.E., Fajardo, O., Matsue, H., Anderson, R.G., and Lacey, S.W. (1995). Folate receptors targeted to clathrin-coated pits cannot regulate vitamin uptake. Proc. Natl. Acad. Sci. USA *92*, 3824–3828.

Rohatgi, R., Ho, H.Y., and Kirschner, M.W. (2000). Mechanism of N-WASP activation by CDC42 and phosphatidylinositol *4*, 5-bisphosphate. J. Cell Biol. *150*, 1299–1310.

Skretting, G., Torgersen, M.L., van Deurs, B., and Sandvig, K. (1999). Endocytic mechanisms responsible for uptake of GPI-linked diphtheria toxin receptor. J. Cell Sci. *112*, 3899–3909.

Sonnichsen, B., De Renzis, S., Nielsen, E., Rietdorf, J., and Zerial, M. (2000). Distinct membrane domains on endosomes in the recycling

pathway visualized by multicolor imaging of Rab4, Rab5, and Rab11. J. Cell Biol. *149*, 901–914.

Taraboulos, A., Scott, M., Semenov, A., Avrahami, D., Laszlo, L., Prusiner, S.B., and Avraham, D. (1995). Cholesterol depletion and modification of COOH-terminal targeting sequence of the prion protein inhibit formation of the scrapie isoform. J. Cell Biol. *129*, 121–132.

Tooze, J., and Hollinshead, M. (1991). Tubular early endosomal networks in AtT20 and other cells. J. Cell Biol. *115*, 635–653.

Varma, R., and Mayor, S. (1998). GPI-anchored proteins are organized in submicron domains at the cell surface. Nature *394*, 798–801.

Vogel, U., Sandvig, K., and van Deurs, B. (1998). Expression of caveolin-1 and polarized formation of invaginated caveolae in Caco-2 and MDCK II cells. J. Cell Sci. *111*, 825–832.

West, M.A., Prescott, A.R., Eskelinen, E.L., Ridley, A.J., and Watts, C. (2000). Rac is required for constitutive macropinocytosis by dendritic cells but does not control its downregulation. Curr. Biol. *10*, 839–848.